The dispersion of marked fluid in turbulent shear flow

By J. W. ELDER†
Cavendish Laboratory, University of Cambridge

(Received 24 September 1958)

The analysis used by Taylor (1954) and based on the Reynolds analogy has been extended to describe the diffusion of marked fluid in the turbulent flow in an open channel. The coefficient of longitudinal diffusion arising from the combined action of turbulent lateral diffusion and convection by the mean flow is computed to be $5{\cdot}9u_\tau h$, where h is the depth of fluid and u_τ the friction velocity. This is in agreement with experiments described herein. The lateral diffusion coefficient is found by experiment to be $0{\cdot}23u_\tau h$, which is three times larger than the value obtained by the assumption of isotropy. The same analysis can be used to describe the longitudinal dispersion of discrete particles, both of zero buoyancy and of finite buoyancy, and comparison is made with observations by Batchelor, Binnie & Phillips (1955) and Binnie & Phillips (1958).

1. Introduction

This paper describes the application of the analysis used by Taylor (1953, 1954), in his work on diffusion in a circular pipe, to the case of turbulent flow in a wide channel with a free surface. For pipe flow, fluid particles are laterally restrained, whereas in such a channel this is not so. This extra degree of freedom allows a direct investigation of the validity of the assumptions made by Taylor in calculating the small contribution to the longitudinal dispersion due to longitudinal turbulent diffusion. The investigation is of some practical importance in connexion with the disposal of industrial wastes and particularly of radioactive material in estuaries and the ocean.

At the present time there are two general approaches to the problem of diffusion. The first is the Lagrangian approach, an essentially kinematic formulation originally developed by Taylor (1922) in his theory of continuous movements. A recent survey has been given by Batchelor & Townsend (1956). The second method uses a Eulerian formulation and is the method used in the calculation below. This calculation is identical in principle to that used by Taylor (1954) for longitudinal diffusion in a pipe. It relies on the fact that the flow in a pipe or channel, under the action of a steady pressure gradient, is statistically steady and a function of a single co-ordinate y only. The dispersion process is controlled by the combined action of the longitudinal convection of fluid elements

† Present address: Department of Scientific and Industrial Research, Wellington, New Zealand.

at speeds depending on their lateral positions, and the lateral diffusion of fluid elements produced by turbulent mixing or molecular diffusion.

Consider the dispersion of those fluid particles which are labelled at some initial instant by injecting a dye or solute into the flow. The resulting mixture of fluid and dye is assumed to be of the same density ρ and kinematic viscosity ν as the original fluid, and the dye particles are assumed to be of zero size. Particles of finite size are discussed in § 5. Thus we have a solute which is hydrodynamically indistinguishable from the channel fluid. For this reason the term self-diffusion has much to recommend it. The process of diffusion we study here is going on all the time in the flow. At the moment of injection we merely label some of the fluid particles so that we may see how fluid particles are being moved about.

A conclusion of some importance immediately follows from the fact that the labelled fluid particles are hydrodynamically indistinguishable from a normal fluid particle. It is that the mean velocity of a marked particle in a pipe or a channel is the same as the discharge velocity; because the discharge velocity is the average particle velocity taken over all realizations of the flow. Alternatively, the result follows the fact that the probability of a particle passing through an element of area of a given flow cross-section is independent of the position of that element on the cross-section. The result was first given by Batchelor *et al.* (1955), who accurately confirmed it by experiments in a circular pipe. Further it is clear that the mean velocity of the centre of mass of a cloud of labelled particles is also equal to the discharge velocity. Since the cloud is made up of many fluid particles, we may expect in practice that even in a single realization (or experiment) the centre of mass will have a velocity very nearly equal to the discharge velocity. This was found to be so by Taylor (1954) in his experiments in a circular pipe and is further confirmed below for the flow in a channel.

Having established the importance of the discharge velocity, it is of interest to see how marked particles are dispersed relative to a point moving with the discharge velocity. Dr G. K. Batchelor pointed out (Taylor 1954) that the original considerations by Taylor for a particle whose velocity is a stationary random function of the time also applied to particles in the statistically steady flow in a pipe or channel. It follows that the mean-square of the fluctuation in (one component of) the position of a fluid particle after a time t is

$$\overline{X^2}(t) = 2\overline{u'^2}\int_0^t (t-p)\,R(p)\,dp, \tag{1}$$

where u' is the fluctuation, about the mean, of the particle velocity, and $R(p)$ is the correlation between $u'(t)$ and $u'(t+p)$. For t sufficiently large to make $R(p) = 0$ the relation becomes

$$\overline{X^2} \to 2\overline{u'^2}\,t\int_0^\infty R(p)\,dp. \tag{2}$$

If an effective diffusion coefficient for the longitudinal dispersion of solute exists, we must have an equation for the rate of change of mean solute concentration of the form

$$\partial S/\partial t = D_1 \partial^2 S/\partial \xi^2,$$

where ξ is a position co-ordinate in the direction of mean flow, relative to an origin moving with the mean velocity of a fluid particle. The solution corresponding to diffusion from an initial concentration at $\xi = 0$ is

$$S = \frac{q}{2(\pi D_1 t)^{\frac{1}{2}}} \exp(-\xi^2/4D_1 t) \quad (q = \text{constant}), \tag{3}$$

for which the dispersion of solute is measured by

$$\int_{-\infty}^{\infty} S\xi^2 \, d\xi = 2D_1 t.$$

This expression has the same t-dependence as (2) and suggests the existence of a diffusion coefficient $\overline{u'^2} \int_0^\infty R(p)\, dp$. The existence of a diffusion coefficient would be proved if it could be shown that the probability distribution of the particle displacement was Gaussian, but such a proof would require a central limit theorem for a stationary continuous process. Although this theorem is not yet available there is widespread belief in its validity. The above analysis is therefore merely suggestive and at the present stage we rely on the experimental observation that the probability distribution of the particle displacement is Gaussian.

2. The longitudinal diffusion coefficient

Consider the dispersion of a solute of neutral particles of concentration s gm/cm^3 of solvent in the steady flow in a channel. Solute is conserved, so that for an incompressible fluid with molecular diffusivity κ,

$$Ds/Dt = \kappa \nabla^2 s.$$

For dispersion in a turbulent velocity field, write $s = S + s'$, $\mathbf{u} = \mathbf{U} + \mathbf{u}'$, where S, $\mathbf{U}$ are mean values of concentration and velocity at a given position, and the fluctuation in velocity is $\mathbf{u}' = (u', v', w')$. Expanding Ds/Dt and averaging the resulting equation with respect to all realizations,

$$DS/Dt + \nabla . (\overline{\mathbf{u}'s'}) = \kappa \nabla^2 S,$$

where from now on D/Dt is the rate of change following the mean motion. Choose a co-ordinate system (x, y, z) so that the x-co-ordinate line is parallel to the mean flow and the mean velocity is a function of y alone. For flow in an open channel of depth h, (x, y, z) are Cartesian co-ordinates, whereas for the flow in a circular pipe of radius h they are cylindrical polars. Components in the directions of the three co-ordinate lines are given subscripts 1, 2, 3, respectively.

It is convenient to define the three diffusivities e_1, e_2, e_3 by

$$\overline{u's'} = -e_1 \partial S/\partial x, \text{ etc.},$$

so that in Cartesian co-ordinates

$$\frac{DS}{Dt} = \frac{\partial}{\partial x}\left(e_1 \frac{\partial S}{\partial x}\right) + \frac{\partial}{\partial y}\left(e_2 \frac{\partial S}{\partial y}\right) + \frac{\partial}{\partial z}\left(e_3 \frac{\partial S}{\partial z}\right) + \kappa \nabla^2 S. \tag{4}$$

For a flow in which the local mean velocity is $U(y)$ the mean concentration S will also be a function of y. In practice this variation is not of primary importance

because of the presence of the channel walls. It is the net diffusive and convective transport longitudinally (x-direction) and the diffusion laterally in the z-direction that is important. To describe this net longitudinal transport we search for a simple solution of the transport equation (4) from which to identify a diffusion coefficient.

Let $e = e_2 + \kappa$ be a given function of y. Consider a distribution of concentration in which no lateral dispersion occurs so that $\partial S/\partial z = 0$. In all cases, terms like $\partial/\partial x$ make only a small contribution to the diffusion coefficient since the marked fluid is extended greatly in the x-direction, so that for the moment they may be neglected. From (4) therefore,

$$y^{-n}\frac{\partial}{\partial y}\left(ey^n\frac{\partial S}{\partial y}\right) = \frac{DS}{Dt}, \tag{5}$$

where $n = 0$ in a two-dimensional channel, $n = 1$ in a circular pipe (Taylor's case), and y is measured from the free surface or the centre of the pipe. Since we are interested in dispersion about a point moving with the discharge velocity $\overline{U}$, write

$$\frac{DS}{Dt} = \frac{\partial S}{\partial t} + \overline{U}\frac{\partial S}{\partial \xi} + U^*\frac{\partial S}{\partial \xi},$$

where $U = \overline{U} + U^*$ and $\xi = x - \overline{U}t$. Seek a solution of (5) for which, since fluid elements are rapidly extended in the x-direction,

$$\frac{\partial S}{\partial t} + \overline{U}\frac{\partial S}{\partial \xi} = 0$$

is a good approximation and the transport of S across a plane at ξ depends only on the small variation of S with y; in this case (5) becomes

$$w^{-n}\frac{\partial}{\partial w}\left(ew^n\frac{\partial S}{\partial w}\right) = h^2U^*\frac{\partial S}{\partial \xi}, \tag{6}$$

where $w = y/h$. Now put $S = P + Q$, where $\partial P/\partial w = 0$, $\partial P/\partial \xi =$ constant, so that the total transport of P across a plane at ξ is zero. If further, following Taylor (1954) and subsequently justifying the procedure by the agreement with measurements, we assume $\partial Q/\partial \xi = 0$, equation (6) is then integrable and we find

$$Q = h^2\frac{\partial P}{\partial \xi}\int_0^w e^{-1}w^{-n}\left(\int_0^w w^nU^*\,dw\right)dw, \tag{7}$$

which satisfies $\partial S/\partial w = 0$ on $w = 0, 1$.

If the longitudinal dispersion can also be described by a diffusion coefficient the rate of transfer of solute across a section of area A at ξ is

$$\int_A U^*Q\,dA \equiv -D_1A\frac{\partial P}{\partial \xi}. \tag{8}$$

The relation (7) then requires

$$D_1 = -h^2\int_0^1 (2w)^nU^*\,dw\left[\int_0^w e^{-1}w^{-n}\left(\int_0^w w^nU^*\,dw\right)dw\right]. \tag{9}$$

This expression applies to both laminar and turbulent flows, provided the time scale of the convective effect is much greater than the time scale of the diffusion of variations of S with y (Taylor 1954). It will also be shown in § 5 to apply to particles of finite size provided U and e are replaced by their mean values over the cross-sectional area of the particle.

3. Turbulent dispersion in an open channel

At the present stage of research it is necessary to deduce the form of the e_i by comparison with experiment. It is fairly well established that near a wall the transfer of momentum and mass are analogous. That is,

$$e_2 = -\overline{v's'}\Big/\frac{\partial S}{\partial y} = -\overline{v'u'}\Big/\frac{\partial U}{\partial y}. \tag{10}$$

This relation will be assumed to hold over the whole channel. For the flow in a channel or pipe in which the velocity field is a function of y only and is otherwise homogeneous, only one such relation (10) can be written down. Hence Reynolds analogy only allows us to calculate directly the longitudinal diffusion coefficient.

For a pipe or channel the Reynolds equations for the mean flow can be integrated to give $\tau = \tau_0 w$, where τ is the stress in the fluid and τ_0 is the stress at the wall. The friction velocity u_τ is defined by $(\tau_0/\rho)^{\frac{1}{2}}$. The velocity distribution satisfies the defect law

$$\left.\begin{aligned} U &= U_1 - u_\tau f(w) \\ \text{and} \qquad \bar{U} &= U_1 - u_\tau \bar{f}, \end{aligned}\right\} \tag{11}$$

where U_1 is the maximum velocity. Hence, by (10) and neglecting the molecular diffusion coefficient which is normally only about $10^{-4} e_2$,

$$e = h u_\tau w / f'. \tag{12}$$

The velocity distribution is specified by the function $f(w)$. Taylor, in his calculation for dispersion in a pipe, used an empirical function based on experiment. For flow in an open channel $f(w)$ is given closely by the logarithmic law of the wall

$$kf(w) = -\log(1-w), \tag{13}$$

where $k = 0{\cdot}41$ is an absolute constant.

Hence D_1 is determined by (11), (12), (13) and (9) and for $n = 0$ the first two integrations for D_1 can be performed to give

$$k^3 D_1 / h u_\tau = \int_0^1 w^{-1}(1-w)\,[\log(1-w)]^2\,dw. \tag{14}$$

The integral can be evaluated as a series of gamma functions to give a value $2\sum_{n=2}^{\infty} n^{-3} \doteq 0{\cdot}4041$, so that, on using $k = 0{\cdot}410$, we have

$$D_1 = 5{\cdot}86\, h u_\tau.$$

Turbulent diffusion in the x-direction

So far we have neglected the contribution from the longitudinal turbulent diffusion by ignoring the term $\partial/\partial x(e_1\,\partial S/\partial x)$. Taylor showed that the contribution was normally insignificant for laminar flow and even for turbulent flow was small.

He was able to make a reasonable estimate by assuming $e_1 = e$, which is strictly true in isotropic turbulence. The additional diffusive transport is

$$h\int_0^1 e\frac{\partial S}{\partial \xi}dw \equiv D^*h\frac{\partial S}{\partial \xi}, \tag{15}$$

where D^* is the diffusion coefficient due to the longitudinal turbulent diffusion. Hence

$$D^*/hu_\tau = \int_0^1 w\,dw/f' = k/6 = 0{\cdot}068. \tag{16}$$

The total longitudinal coefficient is thus $(5{\cdot}86 + 0{\cdot}07)\,u_\tau h = 5{\cdot}93\,u_\tau h$. Although the use of the Reynolds analogy by itself does not allow the lateral diffusion coefficient to be calculated, the above calculation for D^* equally well evaluates, on the assumption of isotropy, the diffusion coefficient for lateral diffusion, D_3. Notice that D_3 is linearly related to e, whereas D_1 is linearly related to $1/e$.

4. Experimental results in an open channel

The experimental arrangement

The experimental investigation was performed in the 14-inch water flume of the Engineering Laboratory, Cambridge. The flume is described by Binnie, Davies & Orkney (1955). It was the only suitable channel available in Cambridge, and it severely restricted the range of the experiments. A roof tank was kept full by pumping water from a sink, placed beneath the outlet to the working section. Water from the tank ran through a valve into a reservoir behind the working section. The working section was 10 ft. long, rectangular in section and inclined at 0·046° to the horizontal. A sheet of white, self-adhesive plastic on which had been drawn a grid of black lines spaced 10 cm apart longitudinally and 5 cm apart transversely was stuck to the bottom of the working section.

Turbulent flow did not occur naturally in the channel. Transition to turbulence was stimulated by placing two trip fences of 4 mm height, 20 cm apart, at the beginning of the working section. Dye-injection tests revealed the efficiency of the device. Experiments were always performed more than 50 cm downstream of the trip fences.

The possible experimental range was limited by three factors, the occurrence of waves near Froude number 0·7, the need for the turbulent boundary layer thickness of the flow near the wall to exceed the channel depth and the need for the flow to be turbulent. In the flume used, the inclination was fixed and the weir height was set at zero, since otherwise the experimental range was even more restricted. Then U_1 is an increasing function of h. In the channel used here, $U_1 = 23h^{0{\cdot}63}$ cm/sec, for h in cm. The mean velocity profile was determined with a total head tube and an inclined tube manometer. The profile was directly confirmed to be the same throughout the working section. All the profiles measured satisfied (13), except very near the wall and very near the surface, for $h < 1{\cdot}5$ cm. Thus the experiments were limited to a depth of 1·0 to 1·5 cm, corresponding to a Reynolds number range of 2300 to 4500. The viscous sublayer caused departures from a logarithmic profile for $w < 0{\cdot}05$. The friction velocity

determined from the experimental profiles agreed to within $\pm 1\,\%$ with values obtained by using a Reynolds number based on the so-called hydraulic mean depth and pipe data for the friction velocity (Nikuradse 1930). Over the range considered here

$$\overline{U}/u_\tau = 5{\cdot}09(\overline{U}h/\nu)^{\frac{1}{8}}.$$

The depth of flow was determined with a pricker gauge and the discharge velocity from the rate of discharge of water volume at the end of the channel.

It was not permissible to use salt as the solute because the recirculated water was also used in other machines in the Laboratory, but permanganate solution is both harmless and intensely coloured. A stock solution was made up to a density $1{\cdot}033\,\mathrm{g/cm^3}$. Normally measurements encountered concentrations smaller by a factor 10^{-3} to 10^{-4}. Most of the measurements were made photographically. The working section was uniformly illuminated through the glass sides, photographed from above on Ilford FP3 film and developed in Ergol at 25 °C to a Weston rating of 400. This allowed a short exposure time and fine grain. Conditions of illumination, exposure and development were carefully standardized. Up to 80 strip photographs could be obtained on a single film. Each film was directly calibrated first by taking a photo with no dye in the channel, and secondly with a series of pots, filled with dye of known concentration, placed in the channel.

The film blackness is described by the density $d = -\log_{10} T$, where T is the proportion of light transmitted through the film. Over a considerable portion of the film characteristic there is a linear relation between d and the logarithm of the exposure. For a fixed exposure time the exposure is proportional to the intensity of illumination which the camera is viewing. Let the illumination with no dye in the channel be I_0. Hence if the light scattering is small and the presence of dye does not alter I_0, the observed illumination I is given by the usual relation

$$I = I_0 \exp\left(-\beta \int_0^h s\,dy\right),$$

where s is the instantaneous concentration, β is a constant related to the particular dye and the channel fluid, and it is assumed that the camera is at infinity in the y-direction. When the film is read we obtain Δd, the difference of density between that with dye in the flow and that without dye in the flow. Hence

$$\Delta d \propto C, \quad \text{where} \quad C = \int_0^h s\,dy.$$

The relation between concentration C and density was linear up to $\Delta d = 0{\cdot}7$, and although allowance was made for the non-linearity of this relation it was normally quite small. As the bulk of the observations had a density of less than 0·5, corrections due to non-linearity were not often used. The film was automatically read and plotted on the J.L.C. Walker Microdensitometer of the Medical Research Unit, Cavendish Laboratory. Normally the instrument was used with $d = 0{\cdot}5$ corresponding to the full scale of 19 cm. Plotting reproducibility was $\pm 0{\cdot}2$ mm.

There is an important advantage of the photographic or fixed time method over probe or fixed distance method. If the diffusion rate is high, the concentration

distribution may change sufficiently quickly while the cloud is passing over a probe to produce a long tail (Levenspiel & Smith 1957). Consider the simple example of injecting a small volume q of dye at unit concentration at $t = 0$ into a pipe of unit cross-section in which the fluid has a discharge velocity $\overline{U}$. At a later time the concentration is given by (3). For observations at $x = X$, S is not a Gaussian function of time unless $X^2/Dt \doteqdot \overline{U}X/D$ is large. Even for $\overline{U}X/D = 50$ a tail twice as long as for a Gaussian curve is found. In my experiments this corresponds to $X \doteqdot 40$ cm. Thus the use of the photographic method in this experiment is very desirable.

The method of injecting the dye was designed to be as simple and reproducible as possible. For continuous injection a constant head of dye was maintained above a 1·0 mm circular jet. The wall of the jet was held 1 mm from the surface so

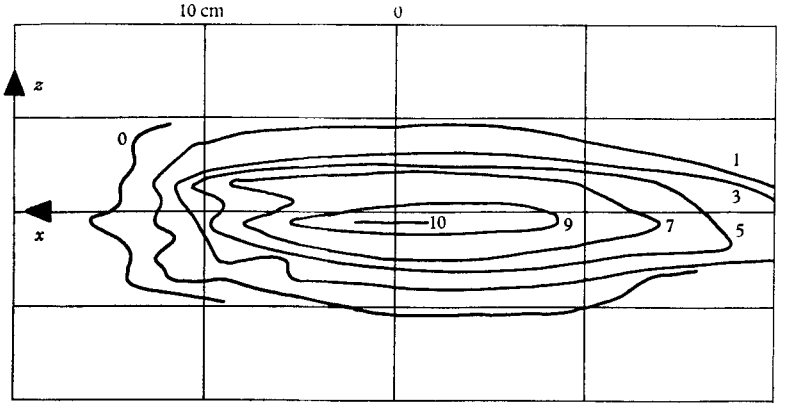

FIGURE 1. Plan view of a drop of dye diffusing in the turbulent flow in an open channel. Distribution of concentration C, normalized to have a maximum of 10. The flow is to the left. $h = 1{\cdot}43$ cm, $X/h = 90$.

that the dye was injected normal to the surface at a rate between 0·1–0·4 cm^3/sec. For the injection of drops a tube of 4 mm internal diameter was attached to a small chamber ending in a rubber diaphragm. A 1 cm length of the tube was filled with dye and the tube end held 1 cm from the surface. When the diaphragm was tapped the dye was shot into the water in the channel.

The experimental results

If a drop of dye is injected and observed at some later time the drop appears as shown in figure 1. Lines of equal values of the concentration C, with a maximum of 10, are shown. The longitudinal dispersion is some 5 times the lateral dispersion. The curves are much more disturbed in front and a pronounced tail is seen behind.

The mean position of the drop averaged over all realizations was directly verified to correspond to the position of a point moving with the discharge velocity to better than the experimental accuracy of 0·2 %. First, direct observations were made with a stop-watch, giving an accuracy over several runs of $\pm$ 0·1 sec in about 10 sec. Secondly, at the same instant as the drop of dye was released, a stop-watch was started and also a piece of paper, 2 cm in diameter, was placed on the water surface at a known position some distance upstream of the

injection point. The piece of paper moves downstream with the surface velocity. At a later time a photograph was taken showing the stop-watch, the piece of paper and the diffusing drop. The shutter speed was 0·003 sec. The accuracy is now determined by the measurements of a small length in a total length of 350 cm. No significant departure from the assumption could be found.

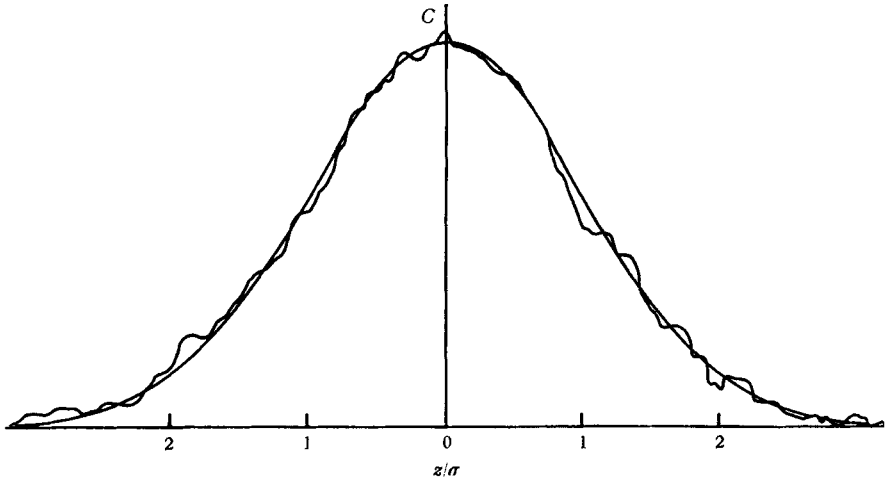

FIGURE 2. Lateral concentration distribution across the middle of a diffusing drop and the Gaussian curve of best fit. $h = 1{\cdot}34$ cm, $X/h = 110$, σ = standard deviation.

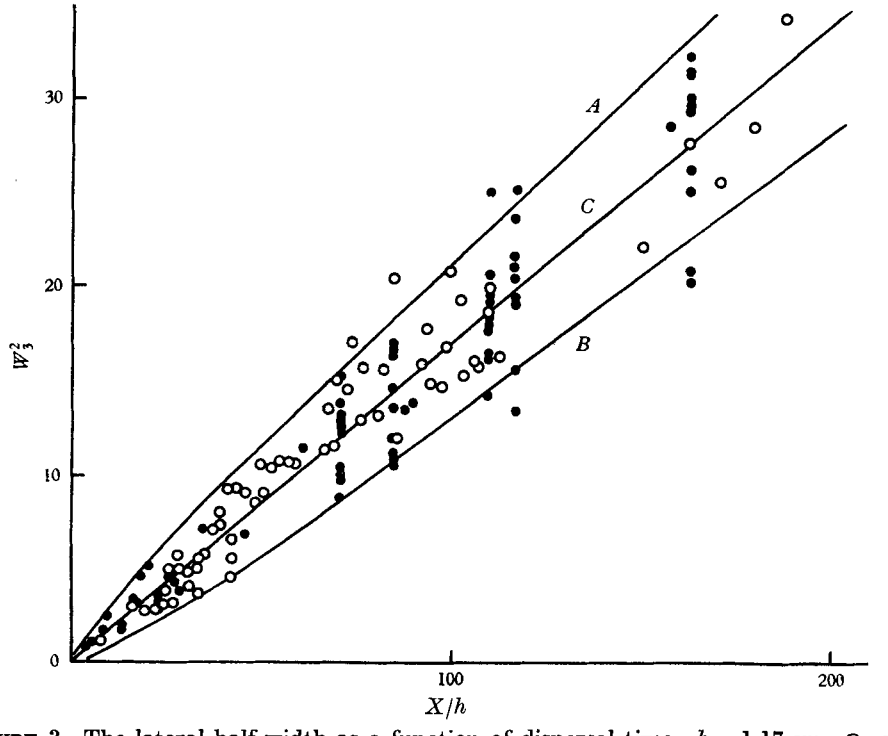

FIGURE 3. The lateral half-width as a function of dispersal time. $h = 1{\cdot}17$ cm; ○, continuous injection; ●, drop injection. *A*, *B*, *C* correspond to $w_3 = 0{\cdot}5$, $-0{\cdot}5$, 0, where $W_3 = \overline{W}_3 + w_3$.

Figure 2 shows a direct tracing of a microdensitometer traverse laterally across the middle of such a drop together with the Gaussian curve of best fit. The variations are directly due to variations of the concentration in the stream and are not due to grain on the film. The closeness of fit even in the tails is remarkable. Evidently the lateral dispersion can be described by a diffusion coefficient since a Gaussian distribution of concentration implies the existence of a diffusion coefficient. Figure 3 shows that the diffusion coefficient is independent of X for large X, where X is the mean position of the drop at any instant, this figure (based on 133 measurements both from drops and continuous injection) gives experimental values of W_3^2 as a function of X, where

$$W_3 = (\text{lateral half-width})/h,$$

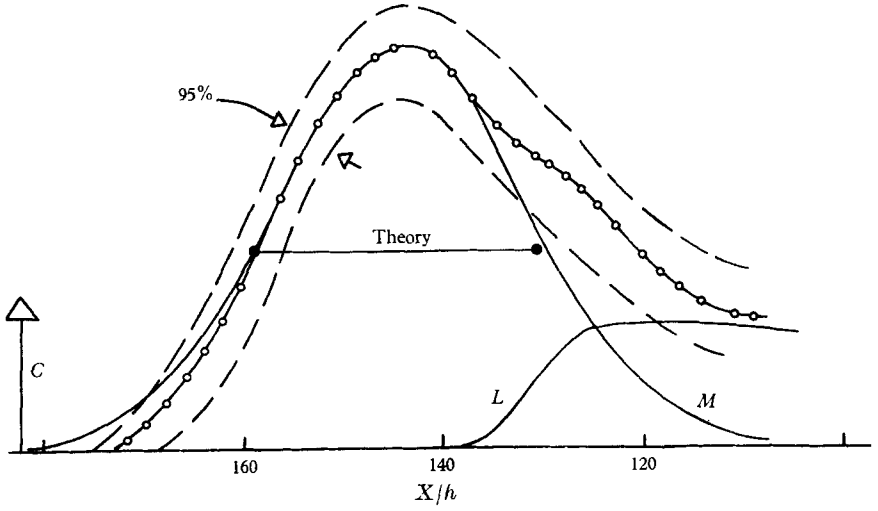

FIGURE 4. The mean longitudinal concentration distribution and the 95 % limits along the centre line of a diffusing drop. $h = 1{\cdot}27$ cm, $R = 3{\cdot}41 \times 10^3$. M, turbulent component; L, sublayer component.

and the half-width is the distance between the points at which the concentration is half the maximum value. The points lie about a mean line C for which $\overline{W_3^2} \propto X/h$, corresponding to a lateral diffusion coefficient $D_3 = 0{\cdot}228 u_\tau h$, about three times the value given by (16). If we write $W_3 = \overline{W}_3 + w_3$, the lines A, B, C correspond to $w_3 = 0$, $\frac{1}{2}$, $-\frac{1}{2}$ respectively. The probability distribution of w_3, $P(w_3)$, is symmetrical about $w_3 = 0$, has a standard deviation of 0·204, and at $w_3 = 0{\cdot}05$, 0·15, 0·25, 0·35, 0·45, 0·60 has the values $P(w_3) = 0{\cdot}119$, 0·119, 0·109, 0·072, 0·050, 0·018. $P(w_3)$ is much more rectangular than Gaussian. Notice that w_3 is independent of X so that the proportional scatter decreases as $X^{-\frac{1}{2}}$. Even at $X/h = 100$ the scatter is ± 5 % S.D.

The longitudinal dispersion can also be described by a diffusion coefficient. From the photographs, taken at the same dispersion time, from 20 different drops, a mean and a 95 % concentration curve have been derived from traverses along the centre line of the drop, and are shown in figure 4. The 95 % curve defines the region outside which 5 % of the points lie. The mean curve can be considered to consist of two components. The first and main component corresponds to solute

which is being carried in the fully turbulent part of the channel, whereas the second component arises from solute which is being carried near the wall in the viscous sub-layer. Since $C = \int_0^h s\,dy$, the total observed concentration is the sum of the two concentrations. In figure 4 an attempt has been made to separate the two components into a Gaussian curve, M, and another curve, L, by obtaining as good a fit as possible to the Gaussian curve over the forward portion of the experimental curve. From this Gaussian curve we obtain the experimental value 6·3 for D_1/hu_τ, about 8 % higher than that given by the calculation. The measurements were made at a Reynolds number of $3{\cdot}5 \times 10^3$. At such low Reynolds numbers it has already been noticed by Taylor (1954) that experimental values exceed those of calculation. The longitudinal half-width ($= W_1 h$) is given in figure 5 as a function of X/h. For the larger values of X/h the behaviour is similar to that of the lateral half-width. Writing $W_1 = \overline{W}_1 + w_1$, lines A, B, C in the figure correspond to $w_1 = 1, -1, 0$. The standard deviation of w_1 is 0·48, some 2·4 times larger than for the lateral scatter.

Notice that (figure 4) the distribution of concentration in the sublayer component L quickly rises to a peak, at a distance of about $2(2D_1 t)^{\frac{1}{2}}$ upstream of the centre of the drop, beyond which a long tail extends upstream. It is possible to obtain experimental values of the ratio of the length scales of the L and M distributions by comparing the distances between the maxima and the upstream point at which the concentration C has dropped to half its maximum value. This ratio was found to lie between 5 and 7 for the data of figure 4.

Departures from the simple theory due to the eddy structure

The most novel feature of the observations presented above is the simple manner in which the half-width for each realization varied about the mean half-width. If $W = \overline{W} + w$, the probability distribution of w, $P(w)$, is symmetrical about $w = 0$ and independent of W or X. For the lateral half-width the standard deviation of w_3 was 0·20. Thus ± 3 standard deviations extend over a width of $1{\cdot}2h$. The photographs show that the edge of the drop is distorted on a scale of order h. Thus we identify the spread of W as due to large eddy motions whose planes of circulation extend over an appreciable portion of the channel depth. These large eddies have been studied recently by Grant (1958). Similar remarks apply to the variation in the longitudinal width.

Taylor's expression (1) can be written as

$$\overline{X^2} = A_1 t - B_1,$$

where, as $t \to \infty$,

$$A_1 \to 2\overline{u'^2} \int_0^\infty R(p)\,dp, \quad B_1 \to 2\overline{u'^2} \int_0^\infty pR(p)\,dp,$$

with similar expressions relating the mean-square particle displacement in the y- and z-directions, $\overline{Y^2}$, $\overline{Z^2}$, to A_2, B_2 and A_3, B_3. Using this relation to extrapolate the data of figures 3 and 5 shows that for lateral diffusion $|B_3| < 0{\cdot}05h^2$, and for longitudinal diffusion $B_1 \doteqdot 30h^2$. The small value of B_3 suggests that the Lagrangian correlation $R_{33}(0, 0, t)$ reverses sign while the large value of B_1 suggests that

$R_{11}(t, 0, 0)$ is of constant sign and very extensive. This behaviour is seen to be similar to that of the corresponding Eulerian correlations recently measured by Grant (1958) in a boundary layer and suggests that the eddy motions responsible for these correlations persist for a considerable time.

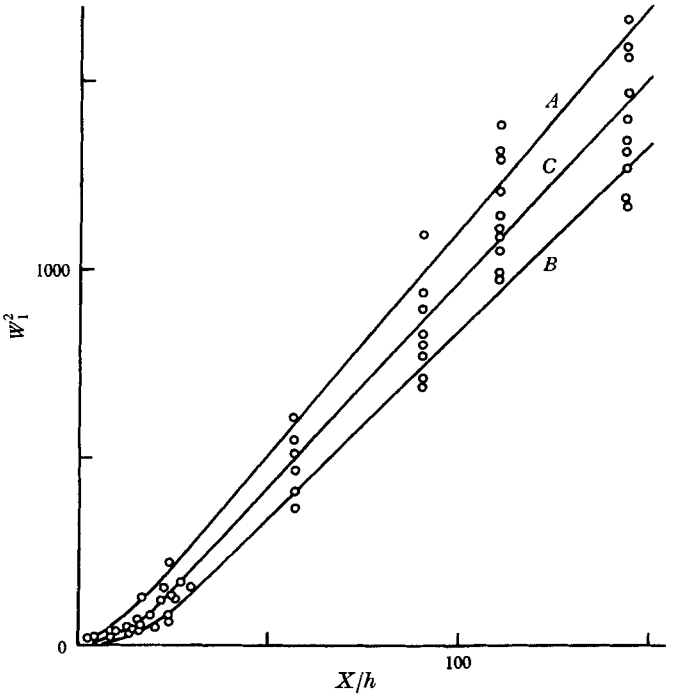

FIGURE 5. The longitudinal half-width as a function of dispersal time. $h = 1{\cdot}27$ cm. A, B, C corresponds to $w_1 = 1, -1, 0$, where $W_1 = \overline{W}_1 + w_1$.

Departures from the simple theory due to the wall sublayer

It is already well known that the distribution of concentration is found experimentally to be asymmetric for small Reynolds number and small dispersal time. I have mentioned that this can occur due to observations being made at a fixed point, at small values of $\overline{U}X/D$. This spurious effect is not responsible for the long tails found by Taylor (1954) in experiments in which $\overline{U}X/D \gg 100$. Nor, of course, does it apply to the present method. But we have so far considered the channel as completely filled by fully turbulent motion and have ignored the influence of the flow in the viscous sublayer next to the wall. This layer extends to

$$y_s/h \doteqdot 10\nu/u_\tau h = 50R^{-\frac{7}{8}},$$

at which position the mean velocity is

$$U_s/U_1 \doteqdot 10u_\tau/U_1 = 2R^{-\frac{1}{8}}.$$

Subscripts s refer to the edge of the sublayer, $R = U_1 h/\nu$ and $U_1/u_\tau \doteqdot 5R^{\frac{1}{8}}$. It seems reasonable to assume that the flow field is sharply divided into laminar and turbulent regions by the sublayer surface at $y = y_s$ and that marked particles can be exchanged between the two regions only by molecular diffusion. We have

already seen that a diffusion coefficient can be defined in the turbulent region. The same method can by employed to calculate the value of the diffusion coefficient D_s appropriate to the linear velocity profile of the sublayer (Couette flow). It is easily shown from (9) that $D_s = y_s^2 U_s^2/120\kappa$.

Thus the two layers can both be described by diffusion equations. The diffusion in the turbulent layer occurs about a point moving with the discharge velocity $\overline{U}$, but the diffusion in the sublayer occurs about a point moving with the velocity $\frac{1}{2}U_s$. While a diffusing drop is passing over a point in the sublayer, marked particles enter the sublayer, and as the drop passes downstream these particles disperse, by longitudinal dispersion in the sublayer and by molecular diffusion back across the sublayer surface into a well-stirred region of nearly zero concentration.

The derivation of the form of D_s relies on the assumption that the rate of transport of solute in the y-direction, and in particular the transport of solute across the plane $y = y_s$ is small compared with the transport longitudinally (Taylor 1954). That this is normally the case is seen by noting that the time for a particle in the sublayer to move (by molecular diffusion) a distance y_s in the y-direction is $y_s^2/2\kappa$, a time much larger than even the total dispersion time available in the present experiments.

The assumption that the transport of solute across y_s out of the sublayer has a much smaller effect on the distribution of solute in the sublayer, once the turbulent cloud has passed, than longitudinal dispersion in the sublayer, is supported by a comparison of the measured length scale of the tail with values computed from D_s. It is convenient to do this by comparing the length scale of the longitudinal dispersion in the turbulent layer, X_1, with the length scale of that in the sublayer, X_s. We have for the ratio of these length scales $X_s/X_1 = (D_s/D_1)^{\frac{1}{2}}$; but

$$D_1/\nu = 1{\cdot}16R^{\frac{7}{8}}, \quad D_s/\nu = \left(\frac{y_s}{h}\right)^2 \left(\frac{U_s}{U_1}\right)^2 \frac{R^2}{120\kappa} = 83\,\nu/\kappa,$$

so that

$$X_s/X = 8{\cdot}6R^{-\frac{7}{16}}(\nu/\kappa)^{\frac{1}{2}}.$$

For the data of figure 4 we have $R = 3{\cdot}4 \times 10^3$, $\kappa = 1{\cdot}5 \times 10^{-5}\,\mathrm{cm}^2/\mathrm{sec}$ and therefore $X_s/X_1 = 6{\cdot}3$. Experimental values lay between 5 and 7. This verification of the assumption of the independence of the two layers provides some justification of the analysis of the data of figure 4 into two components.

The isotropic assumption

The isotropic assumption involved in calculating the lateral diffusion is in error by a factor of 3. Particles disperse laterally some 70 % faster than for the isotropic case. It was to be expected that the isotropic assumption produces too low a value of D_3, since the lateral turbulent intensity always exceeds the vertical intensity ($\overline{w'^2} - \overline{v'^2} \doteq \tau_0/\rho$; see Klebanoff 1954). It may therefore be supposed that the contribution of the turbulent fluctuating motion to the longitudinal dispersion is also in error. Assume that this contribution equals the lateral diffusion coefficient, thus giving $D_1 = (5{\cdot}86 + 0{\cdot}23)\,hu_\tau = 6{\cdot}1hu_\tau$, with $D_3 = 0{\cdot}23u_\tau h$. The experimental value of D_1, viz. $6{\cdot}3hu_\tau$, about 3 % high, is in reasonable agreement with theory, despite unfortunately low values of the Reynolds number and small dispersion times imposed by the apparatus.

5. The dispersion of discrete particles

The dispersion of non-buoyant particles

Before analysis similar to that of § 2 can be applied to the dispersion of finite solid particles of radius αh it is necessary to establish the appropriate form of both the particle velocity and the particle diffusivity. First, the mean velocity of discrete particles in the flow in a circular pipe has been shown by Batchelor *et al.* (1955)—and in an extension of the investigation by Binnie & Phillips (1958)—to be given accurately, provided α is less than about 0·15, by the discharge velocity obtained from the discharge due to the part of the pipe cross-section that is accessible to the particle centre. For larger particles ($0{\cdot}15 < \alpha < 0{\cdot}3$) it was found to be more accurate to estimate the mean particle speed on the assumption that the velocity of the particle, when its centre is at position y, is equal to the average of the mean fluid speed over a circle of radius αh centred at y. Secondly, in the theory of the transport of suspended sediment (Rouse 1937, and improved by Hunt 1954), the assumption that very small discrete particles ($\alpha \doteqdot 0{\cdot}002$) are dispersed at the same rate as fluid particles leads to good agreement with experiment. Thus we may expect that (9) will also apply to discrete particles, provided some account is taken of the finite size of the particle. The following discussion applies to pipe flow and to particles of size such that $\alpha < 0{\cdot}15$.

The mean particle velocity $\overline{U}(\alpha)$ has to be evaluated over the accessible area $\pi(1-\alpha)^2h^2$ as described above, so that

$$U^*(\alpha,w) = U - \overline{U}(\alpha) = U - \frac{2}{(1-\alpha)^2}\int_0^{1-\alpha} wU\,dw, \tag{17}$$

and this takes the place of U^* in (9).

An estimate of the diffusivity $e(\alpha,w)$ of a particle of finite size can be made by observing that in evaluating (9) the bulk of the contribution to D_1 arises from the region near the wall. In this region the velocity profile is logarithmic, so that by (12) and (13), $e \doteqdot khu_\tau w(1-w)$. Hence,

$$e(\alpha,w) \doteqdot e(0,w) - \tfrac{1}{3}khu_\tau\alpha^2, \tag{18}$$

so that provided α is small the error in writing $e(\alpha, w) = e(0, w)$ is small (the expression does not apply near $w = 0$ or 1). In fact the mean diffusivity $\bar{e}(0) = 4khu_\tau/15$, and the extra term in (18) represents a proportional error of $5\alpha^2/4$.

Observe also that in (8), although D_1 is defined in terms of the transport through an area πh^2, the transport occurs only over an area $\pi(1-\alpha)^2h^2$, so that in (9) the upper terminal of the integral becomes $1-\alpha$.

Equation (9) can be written in the form

$$\left.\begin{aligned} D_1(\alpha) &= -2h^2\int_0^{1-\alpha} wU^*(\alpha,w)\,A(\alpha,w)\,dw,\\ \text{where}\qquad A(\alpha,w) &= \int_0^w (ew)^{-1}\left[\int_0^w wU^*(\alpha,w)\,dw\right]dw, \end{aligned}\right\} \tag{19}$$

$U^*(\alpha, w)$ is given by (17) and $e = e(0,w) = hu_\tau w/f'$ by (12). The function $f(w)$ which defines U by means of (11) has been tabulated by Taylor (1954), and throughout the subsequent calculations we use his values. On performing the integration (17) and writing

$$U^*(\alpha,w) = u_\tau[\bar{f}(0) - f(0,w)] + u_\tau[\bar{f}(\alpha) - \bar{f}(0)], \tag{20}$$

we find
$$A(\alpha,w) = A(0,w) + \frac{1}{2h}[\bar{f}(\alpha) - \bar{f}(0)]f(0,w). \tag{21}$$

The final integration in (19) performed numerically for three values of α gave the values shown below.

α	0 (Taylor)	0·04	0·10	0·15
$\bar{U}(\alpha)$	4·25	3·60	2·98	2·56
$D_1(\alpha)/hu_\tau$	10·1	4·80	2·22	1·21

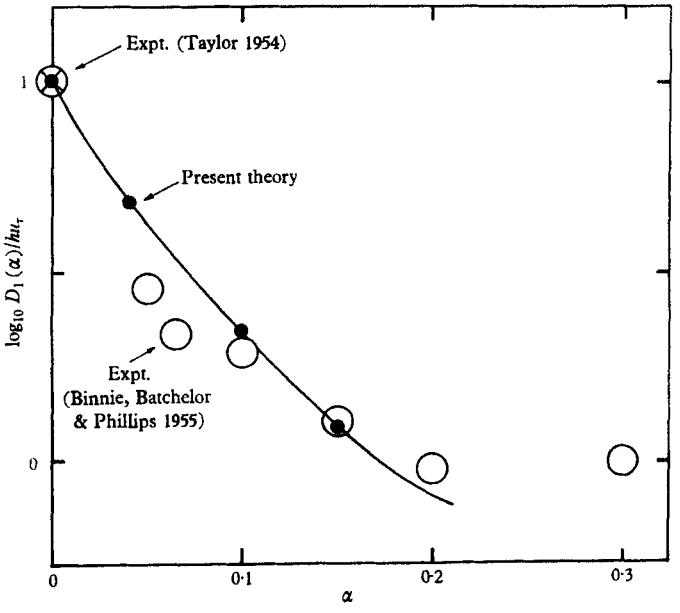

FIGURE 6. Longitudinal dispersion of non-buoyant spheres of radius αh in a circular pipe. Experimental values from Batchelor *et al.* (1955).

These points are shown in figure 6, together with the experimental values obtained by Batchelor *et al.* (1955). The experimental points have a standard error of about 5 %. The radii of the circles correspond to an error of 10 % in D_1. The agreement is quite good. The departure for large α is expected because of the neglect of the curvature of the diffusivity and velocity distributions. The mean error in neglecting the curvature of the diffusivity seems likely to be the greater, and is shown by (18) to be 11 % at $\alpha = 0{\cdot}3$. Thus, for α large, as opposed to the behaviour for α small, the principal effect arises through the diffusivity distribution, and since D_1 is linearly related to $1/e(\alpha,w)$ the neglect of the curvature of $e(\alpha,w)$ as shown by (18) leads to an underestimate of D_1. This is the case for the experimental point at $\alpha = 0{\cdot}3$. There is also significant departure for small values of α. Such an effect has also been observed in Vanoni's (1946) experiments on the transport of suspended sediment. This effect is undoubtedly due to the sublayer near the wall. In this region the tabulated values of $f(w)$ and the computed diffusivity are not necessarily reliable. It should be noticed that the computation of D_1 requires four successive integrations, so that D_1 is sensitive to the form of $f(w)$ and that the bulk of the contribution to D_1 arises near the wall, particularly for the smaller particles. The departure is therefore to be expected.

The dispersion of buoyant and heavy particles

The above discussion applies to particles of density equal to that of the surrounding fluid. In view of the success of the discussion of Binnie & Phillips (1958) in evaluating the mean velocity of buoyant and heavy particles in a circular pipe by means of the hypothesis of sedimentation theory, it appears likely that (9) can again be easily modified to apply to heavy particles. For example, consider the flow in a channel. It is assumed that the probability density $P(w)$ of the position of particles is determined by a balance between the transport due to a settling velocity V and the turbulent transport, so that

$$VP - e\frac{dP}{dy} = 0.$$

This is readily integrated by using (12) and (13) to give

$$P = \left[\frac{w}{1-w}\right]^{\beta} \frac{\sin \pi\beta}{\pi\beta} \quad (\beta \neq 1, 2, \ldots), \tag{22}$$

where $\beta = V/ku_\tau$ (Rouse 1937). The mean particle velocity $\overline{U}(\alpha, \beta)$ is then

$$\overline{U}(\alpha, \beta) = \int_0^{1-\alpha} P(w)\, U\, dw. \tag{23}$$

Equation (9) may now be used as before with $U^* = U - \overline{U}(\alpha,\beta)$ and $e(\beta) = e(0)$.

A rough idea of the variation of D_1 with β can be obtained by considering the artificial example of a parabolic velocity distribution in a channel, in which the probability distribution is given by (22), and the molecular diffusivity is a constant of value κ. From (23) and (9) with $\alpha = 0$ it is easily shown that

$$D_1(\beta) = \frac{U_1^2 h^2}{7560\kappa}(64 + 21\beta - 308\beta^2 - 210\beta^3 - 35\beta^4). \tag{24}$$

$D_1(\beta)$ rises by 0·55 % above $D(0)$ to a weak maximum at $\beta \doteqdot 1/30$ and decreases relatively quickly to zero near $\beta = \pm 0{\cdot}5$. This behaviour is typical only of the very small particles which normally utilize all the available velocity variation across the channel—unless inhibited by buoyancy—so that the convective effect is large and consequently so also is D_1.

For finite particles the available velocity variation is much reduced so that D_1 is less sensitive to buoyancy. Binnie & Phillips (1958) have already evaluated the expression corresponding to (23) for a circular pipe and find

$$\overline{U}(\alpha, \gamma) = (1 - B\gamma^2)\,\overline{U}(\alpha, 0), \tag{25}$$

where $\gamma = V/\overline{U}$ and B is given by their equation (8). For $\alpha = 0{\cdot}1$, $B = 15{\cdot}7$. $D_1(\alpha, \gamma)$ can now be evaluated from (9) and (25) using Taylor's data for $f(w)$. In figure 7, $D_1(\alpha, \gamma)/hu_\tau$ is given for $\alpha = 0{\cdot}1$, together with the experimental values, of accuracy about ± 10 % S.D., obtained by Binnie & Phillips (1958). Theory predicts only a slow change of D_1 with γ, in agreement with experiment. The experiments are not sufficiently accurate to confirm the small theoretical decrease in D_1 with increasing $|\gamma|$ which would be more apparent for smaller values of α.

Thus, it is seen that (9) can be used whenever the velocity and diffusivity distributions of the dispersed entity are known, although the expression is only valid for large dispersal times. The principal departure from the simple theory for small particles occurs at low Reynolds numbers, owing to the effect of the viscous region near the walls.

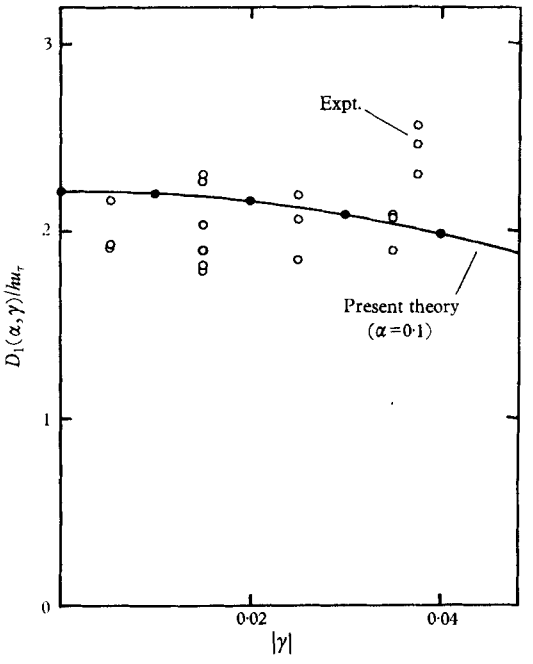

FIGURE 7. Longitudinal dispersion of buoyant and heavy particles in a circular pipe. Experimental values from Binnie & Phillips (1958).

I gratefully acknowledge that my period of research at Cambridge has been made possible by my employers, the New Zealand Defence Scientific Corps.

REFERENCES

BATCHELOR, G. K., BINNIE, A. M. & PHILLIPS, O. M. 1955 *Proc. Phys. Soc.* B, **68**, 1095.

BATCHELOR, G. K. & TOWNSEND, A. A. 1956 Article in *Surveys in Mechanics* (eds. G. K. Batchelor and R. M. Davies). Cambridge University Press.

BINNIE, A. M., DAVIES, P. A. O. L. & ORKNEY, J. C. 1955 *Proc. Roy. Soc.* A, **230**, 225.

BINNIE, A. M. & PHILLIPS, O. M. 1958 *J. Fluid Mech.* **4**, 87.

GRANT, H. 1958 *J. Fluid Mech.* **4**, 149.

HUNT, J. N. 1954 *Proc. Roy. Soc.* A, **224**, 322.

KLEBANOFF, P. S. 1954 NACA Tech. Note 3178.

LEVENSPIEL, O. & SMITH, W. K. 1957 *Chem. Engng Sci.* **6**, 227.

NIKURADSE, J. 1930 *Ing. Arch.* **1**, 306.

ROUSE, H. 1937 *Trans. Amer. Soc. Civ. Engrs*, **102**, 534.

TAYLOR, G. I. 1922 *Proc. Lond. Math. Soc.* (2), **20**, 196.

TAYLOR, G. I. 1953 *Proc. Roy. Soc.* A, **219**, 186; see also **225**, 473.

TAYLOR, G. I. 1954 *Proc. Roy. Soc.* A, **223**, 446.

VANONI, V. A. 1946 *Trans. Amer. Soc. Civ. Engrs*, **111**, 67.